Sensor and Simulation Notes

Note 138

October 1971

A Comparison of the High Frequency-Early Time
Behavior of the Fields Radiated by a Capped
and Uncapped Biconical Antenna

by

M. I. Sancer and A. D. Varvatsis
Northrop Corporate Laboratories
Pasadena, California

Abstract

In this note we compare the early time breaking effect on a radiated
pulse when a finite biconical antenna is either capped or left uncapped.
In the process of making this comparison we also determine the high
frequency diffraction effect for each termination. This problem is studied
by first employing the geometrical theory of diffraction to obtain the high
frequency solution and then the early time solution is derived by taking
the inverse Fourier transform of the diffraction solution. Our results
are summarized by a set of diffraction coefficients that are graphically
presented.

I. Introduction

A pulse-radiating biconical antenna has the property that the early time behavior of the pulse can readily be controlled[1,2]. The first instant that the time behavior of the radiated pulse deviates from the time behavior of the impressed voltage is the instant when the effect of the end of the bicone is felt at the observation point. In this note we compare the effect of two different terminations of the bicone on this initial time deviation. One termination is to cap the bicone with a perfectly conducting plate and the other is to leave the bicone uncapped. Because high frequency and early time solutions are interralated we first direct our attention toward obtaining high frequency corrections to the geometric optics solution of this problem. Since we are interested in the diffraction effect of an edge, we employ the geometrical theory of diffraction[3]. Consequently, in the process of obtaining our early time solution, we obtain the geometrical diffraction solution for this antenna. This solution is of some interest in itself; however, our primary interest is in the early time solution. We obtain this by taking the inverse Fourier transform of the geometrical diffraction solution. The validity of this procedure is discussed in a previous note[4]. Our results appear as a set of two diffraction coefficients, one for the edge nearer to the observation point (upper) and the other for the edge further from the observation point (lower). Each of these coefficients is a tractable function of the bicone angle, the radius of the bicone, the observation angle, and another angle, Ω, which describes the angle of the termination. In this note we consider in detail only the two values of Ω that correspond to the capped and uncapped terminations. A similar analysis to the one contained in this note appears in a previous note[4]; however, the value of Ω was restricted early in the analysis causing the final expressions for the diffraction coefficients to have a more restricted use than those derived in this note.

We summarize our results by a set of four diffraction coefficients, both the upper and lower coefficients for each of the terminations considered. The coefficients for the capped termination are plotted versus the observation angle for four different bicone angles. Also plotted is a ratio indicating

the percentage difference in the diffraction coefficients for the capped and uncapped terminations. Finally, on the same graphs we also present the time that the effect of the terminations will be felt at the observation point.

II. High Frequency Diffraction Field Calculation

The antenna geometry of interest is depicted in figure 1. Our problem is ϕ independent so that we can consider $\phi = 0$ in this figure. Not shown in this figure is the method for terminating the cones. Two different methods for terminating the cones are considered. One is to cap them with a perfectly conducting plate and the other is to leave them uncapped. We assume that the antenna is driven at the common apex of the cones in such a manner that the TEM mode of an infinite biconical antenna is generated. The magnetic field of the TEM mode is used to define the field that is incident on the upper and lower edges, P_U and P_L. For this incident field, the associated rays are all radially directed and consequently they strike the edge of each cone at a right angle. In this situation, the rules governing diffracted rays are such that an incident ray in a constant ϕ plane generates diffracted rays that remain in this plane. A detailed discussion concerning the direction of the diffracted rays can be found in reference 3. We are only interested in the singly diffracted rays that pass through our observation point P. The procedure for determining these rays is also discussed in reference 4 and that procedure will now be applied.

We attach right handed coordinates (T_U, N_U, B_U) and (T_L, N_L, B_L) at P_U and P_L and resolve our incident magnetic field into these coordinates (see figure 2). Our incident magnetic field is given by

$$\underline{H}_i(P_U) = \underline{H}_i(P_L) = h\hat{a}_\phi \qquad (1)$$

where

$$h = \frac{V(\omega)f_o e^{ikd}}{2dZ_o \sin \theta} \qquad (2)$$

$$f_o = \{2 \ln[\cot(\theta_o/2)]\}^{-1} \qquad (3)$$

$$Z_o = \sqrt{\mu_o/\epsilon_o} \qquad (4)$$

4

$$k = \omega\sqrt{\mu_o \varepsilon_o} \qquad . \qquad (5)$$

and $V(\omega)$ is the voltage difference between the two cones as measured along a radial arc. It should be noted that h is half of the total TEM bicone field. The reason is that the total field is equally devided between the incident and reflected fields and it is only the incident that enters into this calculation.

We now resolve the field incident on P_U as

$$\underline{H}_i(P_U) = - h\hat{T}_U \qquad (6)$$

and the field incident on P_L as

$$\underline{H}_i(P_L) = h\hat{T}_L \qquad (7)$$

The reason for the difference in signs is that $\hat{T}_U = - \hat{a}_\phi$ and $\hat{T}_L = \hat{a}_\phi$. The field corresponding to the singly diffracted ray coming from P_U is denoted $\underline{H}_1$ and the field diffracted from P_L is denoted $\underline{H}_2$. The theory leading to the expressions for $\underline{H}_1$ and $\underline{H}_2$ is discussed in reference 4. The explicit expressions are

$$\underline{H}_1 = A(\delta_1,s_1)f(s_1)k^{-\frac{1}{2}} \underline{\underline{D}}_U(\alpha_1,\beta_1,\gamma_1) \cdot \underline{H}_i(P_U) \qquad (8)$$

an l

$$\underline{H}_2 = A(\delta_2,s_2)f(s_2)k^{-\frac{1}{2}} \underline{\underline{D}}_L(\alpha_2,\beta_2,\gamma_2) \cdot \underline{H}_i(P_L) \qquad (9)$$

where

$$A(\delta,s) = \left|1 - (s/a)\cos \delta\right|^{-\frac{1}{2}} \qquad (10)$$

$$f(s) = s^{-\frac{1}{2}} e^{iks} \qquad (11)$$

5

$$\underline{\underline{D}} = B\underline{\underline{W}} \tag{12}$$

$$B = \lambda e^{i\pi/4} (2\pi)^{-\frac{1}{2}} \sin \lambda\pi \quad . \tag{13}$$

$$\lambda = 1/2(1 - \Omega/\pi)^{-1} \tag{14}$$

$$\underline{\underline{W}} = \begin{bmatrix} U + V & 0 & 0 \\ (U + V)\cot \gamma \sin \beta & -(U - V)\cos \alpha \cos \beta & (U - V)\sin \alpha \cos \beta \\ (U + V)\cot \gamma \cos \beta & (U - V)\cos \alpha \sin \beta & -(U - V)\sin \alpha \sin \beta \end{bmatrix} \tag{15}$$

$$U = (\cos \lambda\pi - \cos \lambda(\pi - \beta + \alpha))^{-1} \tag{16}$$

$$V = (\cos \lambda\pi + \cos \lambda(\pi - \beta - \alpha))^{-1} \tag{17}$$

$\underline{\underline{W}}_U$ is defined by considering the rows and columns of $\underline{\underline{W}}$ to be ordered as $\hat{T}_U$, $\hat{N}_U$, $\hat{B}_U$ and $\underline{\underline{W}}_L$ is defined by considering them to be ordered $\hat{T}_L$, $\hat{N}_L$, $\hat{B}_L$. It now remains to define α_1, β_1, δ_1, γ_1, and s_1 as well as α_2, β_2, δ_2, γ_2, and s_2. These quantities are depicted in figure 2. In this figure we allow for a general termination angle Ω and the dashed lines used to define Ω correspond to a hidden cone of metal if $\Omega < \pi/4 - \theta_0/2$. The capped bicone corresponds to $\Omega = \pi/4 - \theta_0/2$ and the uncapped bicone corresponds to $\Omega = 0$. The problem treated in a previous note[4], that of the bicone feeding a cylinder corresponds to $\Omega = (\pi - \theta_0)/2$. The formulas presented in that note are not valid for a general Ω because Ω was set equal to $(\pi - \theta_0)/2$ before general results were presented. The expressions now presented are valid for a general Ω.

$$\alpha_1 = \pi - \Omega \tag{18}$$

$$\beta_1 = \pi + \xi_1 - \Omega - \theta_0 \tag{19}$$

6

$$\xi_1 = \begin{cases} \pi - \arctan(\dfrac{r \sin \theta - a}{L - r \cos \theta}) & L > r \cos \theta \\[2mm] \arctan(\dfrac{r \sin \theta - a}{r \cos \theta - L}) & r \cos \theta > L \end{cases} \qquad (20)$$

$$\delta_1 = \pi/2 + \tau_1 \qquad (21)$$

$$\tau_1 = \arctan(\dfrac{r \sin - a}{|L - r \cos \theta|}) \qquad (22)$$

$$\gamma_1 = \pi/2 \qquad (23)$$

$$s_1 = (r^2 + d^2 - 2r(a \sin \theta + L \cos \theta))^{\frac{1}{2}} \qquad (24)$$

$$\alpha_2 = \pi - \Omega \qquad (25)$$

$$\beta_2 = 3\pi/2 + \xi_2 - \Omega - \theta_o \qquad (26)$$

$$\delta_2 = \pi - \xi_2 \qquad (27)$$

$$\xi_2 = \arctan(\dfrac{L + r \cos \theta}{r \sin \theta - a}) \qquad (28)$$

$$\gamma_2 = \pi/2 \qquad (29)$$

$$s_2 = (r^2 + d^2 + 2r(L \cos \theta - a \sin \theta))^{\frac{1}{2}} \qquad (30)$$

All of the quantities needed to determine $\underline{H}_1$ and $\underline{H}_2$ as given by (8) and (9) have now been defined. The diffracted field corresponding to $\underline{H}_1$ and $\underline{H}_2$ is

$$\underline{H}_D = H_D \hat{a}_\phi = - H_1 \hat{a}_\phi + H_2 \hat{a}_\phi \tag{31}$$

We obtain the diffracted electric field through the relation

$$\nabla \times H_D \hat{a}_\phi = - i\omega\varepsilon_o E_{\theta D} \hat{a}_\theta \tag{32}$$

or equivalently

$$i\omega\varepsilon_o E_{\theta D} = \frac{\partial H_D}{\partial r} + \frac{1}{r} H_D \tag{33}$$

In order to calculate $E_{\theta D}$ to only as high an order in inverse powers of $k^{\frac{1}{2}}$ as we are permitted in order to be consistent with our calculation of H_D, we will consider only part of the radial derivative term in the right hand side of (33). That is

$$\frac{\partial}{\partial r} f(s_i) = ikf(s_i) \frac{\partial s_i}{\partial r} - \frac{1}{2s_i} f(s_i) \tag{34}$$

and it is only the first term on the right hand side of (34) that can be used in computing $\partial H_D/\partial r$. This leads to

$$E_{\theta D} = Z_o \left[- H_1 \frac{\partial s_1}{\partial r} + H_2 \frac{\partial s_2}{\partial r} \right] \tag{35}$$

where

$$\frac{\partial s_1}{\partial r} = \frac{r-(a \sin\theta + L \cos\theta)}{s_1} \tag{36}$$

$$\frac{\partial s_2}{\partial r} = \frac{r + L \cos\theta - a \sin\theta}{s_2} \tag{37}$$

8

Our resulting expression is

$$E_{\theta D} = \frac{V(\omega) f_o e^{ikd}}{2d \sin \theta_o} B \left\{ A(\delta_1, s_1) g(\alpha_1, \beta_1) (ks_1)^{-\frac{1}{2}} e^{iks_1} \frac{\partial s_1}{\partial r} \right.$$

$$\left. + A(\delta_2, s_2) g(\alpha_2, \beta_2) (ks_2)^{-\frac{1}{2}} e^{iks_2} \frac{\partial s_2}{\partial r} \right\} \qquad (38)$$

where

$$g(\alpha, \beta) = 2(\cos \lambda\pi + \cos \lambda(\Omega - \beta))^{-1} \qquad (39)$$

and the remaining quantities have been previously defined.

III. Early Time Asymptotic Solution

To determine the early time asymptotic solution for $E_{\theta D}$ we take the inverse Fourier transform of (38) for the case where

$$V(\omega) = V_{bo} i/\omega \qquad (40)$$

This corresponds to $V(t) = V_{bo}U(t)$, where $U(t)$ is the unit step function. Substituting (40) into (38) we see that we need only consider the inverse Fourier transform

$$F^{-1}(k^{-\frac{1}{2}} i/\omega e^{iks}) = c^{\frac{1}{2}}e^{i\pi/4}(2/\sqrt{\pi})(t - s/c)^{\frac{1}{2}} U(t - s/c) \qquad (41)$$

where c is the speed of light. Performing the inverse Fourier transform of (38) we obtain

$$E_{\theta D} \sim \frac{f_o V_{bo} Q}{2a} \left\{ (c_1/s_1)^{\frac{1}{2}}(2/\sqrt{\pi})(t^* - t_1)^{\frac{1}{2}} U(t^* - t_1)A(\delta_1, s_1)g(\alpha_1, \beta_1)\frac{\partial s_1}{\partial r} \right.$$

$$\left. + (c_1/s_2)^{\frac{1}{2}}(2/\sqrt{\pi})(t^* - t_2)^{\frac{1}{2}} U(t^* - t_2)A(_2, s_2)g(\alpha_2, \beta_2)\frac{\partial s_2}{\partial r} \right\} \qquad (42)$$

where

$$Q = \frac{\lambda \sin \lambda\pi}{\sqrt{2\pi}} , \quad c_1 = c \times 10^{-9}, \quad t^* = 10^9(t - r/c) \qquad (43)$$

The physical meaning of these t's will now be discussed. The time after the first signal arrives from the origin measured in nanoseconds is t^*. When t^* equals t_1 and t_2 the corresponding contributions arise from single diffraction from P_U and P_L.

We are often interested in considering observation points such that $r \gg d$. When this is the case we obtain the following simplification

$$\beta_1 \simeq \pi + \theta - \Omega - \theta_o, \quad \beta_2 \simeq 2\pi - \theta - \Omega - \theta_o \qquad (44a)$$

$$A(\delta_1, s_1) \simeq A(\delta_2, s_2) \simeq [(r/a)\sin\theta]^{-\frac{1}{2}} \qquad (44b)$$

$$c_1 t_1 = a(\csc\theta_o - \sin\theta - \cos\theta\cot\theta_o),$$

$$c_1 t_2 = a(\csc\theta_o - \sin\theta + \cos\theta\cot\theta_o) \qquad (44c)$$

and when the following quantities appear as multiplicative factors they are approximated as

$$(s_1)^{-\frac{1}{2}} \simeq (s_2)^{-\frac{1}{2}} \simeq r^{-\frac{1}{2}}, \quad \frac{\partial s_1}{\partial r} \simeq \frac{\partial s_2}{\partial r} \simeq 1 \qquad (45)$$

Using (44) and (45) in (42) we obtain

$$rE_{\theta D} \sim \frac{V_{bo}f_o}{\sin\theta}\left\{ D_1(t^* - t_1)^{\frac{1}{2}} U(t^* - t_1) + D_2(t^* - t_2)^{\frac{1}{2}} U(t^* - t_2)\right\} \qquad (46)$$

where

$$D_1 = \frac{\lambda \sin \lambda\pi}{\pi(\cos \lambda\pi + \cos \lambda(\Omega - \beta_1))} \left(\frac{2c_1}{a}\sin\theta\right)^{\frac{1}{2}} \qquad (47)$$

$$D_2 = \frac{\lambda \sin \lambda\pi}{\pi(\cos \lambda\pi + \cos \lambda(\Omega - \beta_2))} \left(\frac{2c_1}{a}\sin\theta\right)^{\frac{1}{2}} \qquad (48)$$

We single out the factor $V_{bo}f_o/\sin\theta$ because it corresponds to the undisturbed infinite bicone electric field. This field should be added to $E_{\theta D}$ in the illuminated region, $\theta > \theta_o$. Our results are contained in D_1 and D_2. We compare these quantities for the case where the bicone is capped, $\Omega = \pi/4 - \theta_o/2$, to the case where the bicone is uncapped, $\Omega = 0$. We denote these quantities as

$$D_{1C} = D_1(\Omega = \pi/4 - \theta_o/2), \quad D_{1U} = D_1(\Omega = 0)$$

$$D_{2C} = D_2(\Omega = \pi/4 - \theta_o/2), \quad D_{2U} = D_2(\Omega = 0) \qquad (49)$$

11

and we plot the magnitudes $\left|D_{1C}\right|$ and $\left|D_{2C}\right|$ versus θ for four different values of θ_o. Because the values of D_{1U} and D_{2U} are close to the values of D_{1C} and D_{2C} we plot the ratios

$$P_1 = 2\left|\frac{D_{1C}-D_{1U}}{D_{1C}+D_{1U}}\right| \tag{50}$$

and

$$P_2 = 2\left|\frac{D_{2C}-D_{2U}}{D_{2C}+D_{2U}}\right| \tag{51}$$

to indicate the percentage difference in the breaking effect due to capping the bicone as compared to leaving it uncapped. Specifically we plot $\left|D_{1C}\right|$, $\left|D_{2C}\right|$, P_1, P_2, t_1, and t_2 versus θ for $\theta_o = 30^o$, 45°, 60°, and 75°. The quantities $\left|D_{1C}\right|$, $\left|D_{2C}\right|$, t_1, and t_2 are plotted for $a = 1$ because the value of these quantities for an arbitrary value of a can then readily be calculated by multiplying $\left|D_{1C}\right|$ and $\left|D_{2C}\right|$ by $a^{-\frac{1}{2}}$ while t_1 and t_2 should be multiplied by a.

12

IV. Summary of Results

In figures 3, 4, 5, and 6 we plot $|D_{1C}|$, $|D_{2C}|$, P_1, P_2, t_1, and t_2 versus θ for $a = 1$ and $\theta_o = 30^\circ$, 45°, 60°, and 75°. We plot P_1 and P_2 to indicate the difference in the diffraction coefficients for the two terminations because the actual difference is difficult to depict graphically. Despite the fact that $|D_{1C}|$, $|D_{2C}|$, P_1, and P_2 are all absolute magnitudes, using the following information one can readily determine the actual values of D_{1C}, D_{2C}, D_{1U}, and D_{2U} from these magnitudes. Both D_{1C} and D_{1U} are positive for $\theta < \theta_o$ and they are negative for $\theta > \theta_o$ while D_{2C} and D_{2U} are negative for all θ. For $\theta < \theta_o$, $D_{1C} > D_{1U}$ while for $\theta > \theta_o$, $|D_{1C}| < |D_{1U}|$. Corresponding to the effect of the lower edge we note that $|D_{2C}| < |D_{2U}|$ for all θ. The signs and ordering of these diffraction coefficients lead us to conclude that the capped termination causes an initially larger total field than the uncapped termination. In the diffraction region, $\theta < \theta_o$, we have only the diffracted field and at t_1 the field corresponding to the capped termination initially becomes larger because $D_{1C} > D_{1U}$. In the illuminated region, $\theta > \theta_o$, and at t_1, again the total field corresponding to the capped termination initially stays larger because $|D_{1C}| < |D_{1U}|$ and a smaller diffracted field is subtracted from the geometric optics field in this region. This shows that the breaking effect of the capped termination in this important region is less than that corresponding to the uncapped termination. These cases are depicted in figure 7. The deviation caused by the lower edge is always less pronounced for the capped termination whether or not we are observing in the illuminated or shadowed region. In either region the field is positive at t_2 and a larger diffracted field must be subtracted from this field corresponding to $|D_{2U}|$ because $|D_{2U}| > |D_{2C}|$ for all θ. The difference between the two terminations tends to decrease as the bicone angle increases.

13
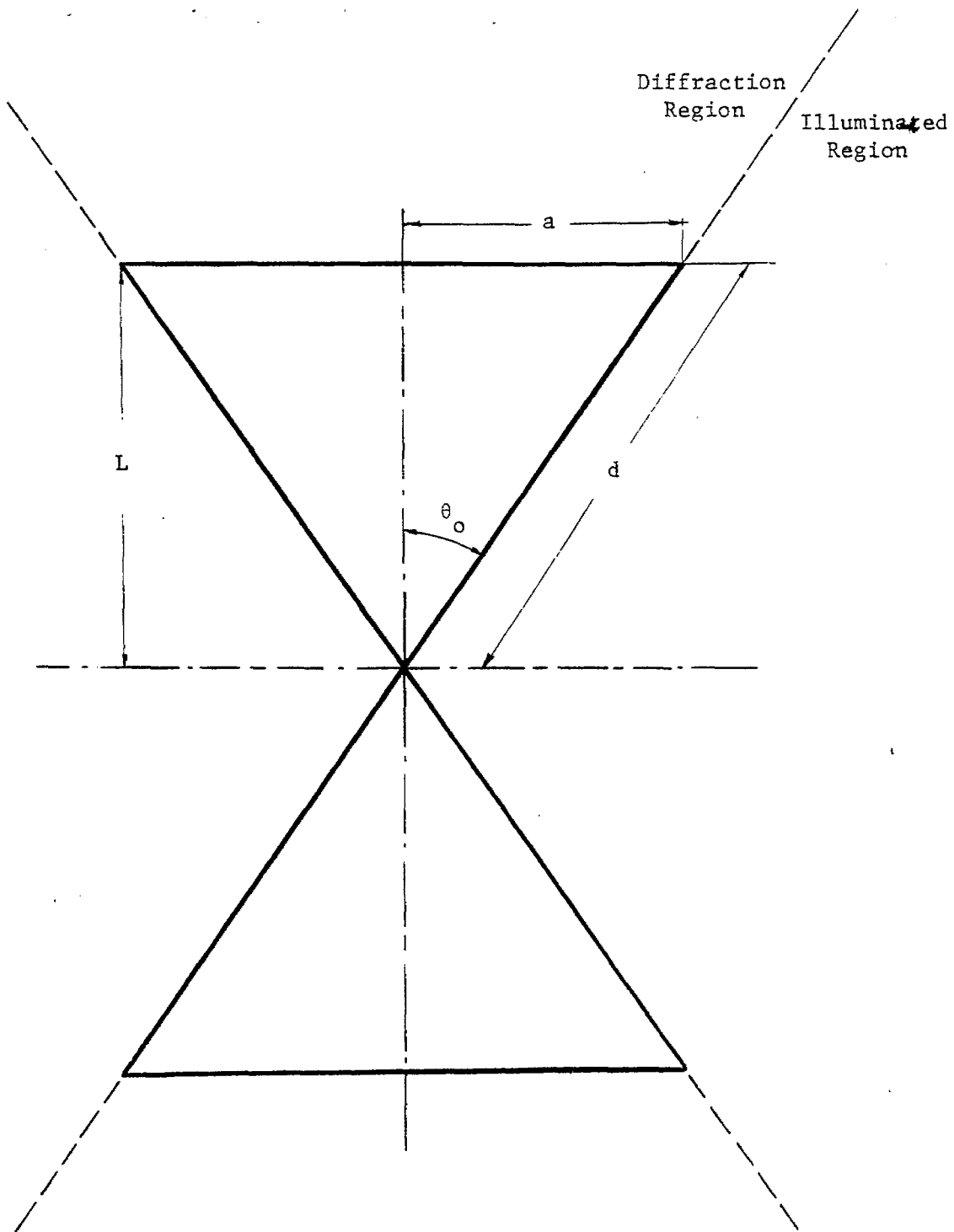
Figure 1.   Antenna Geometry.
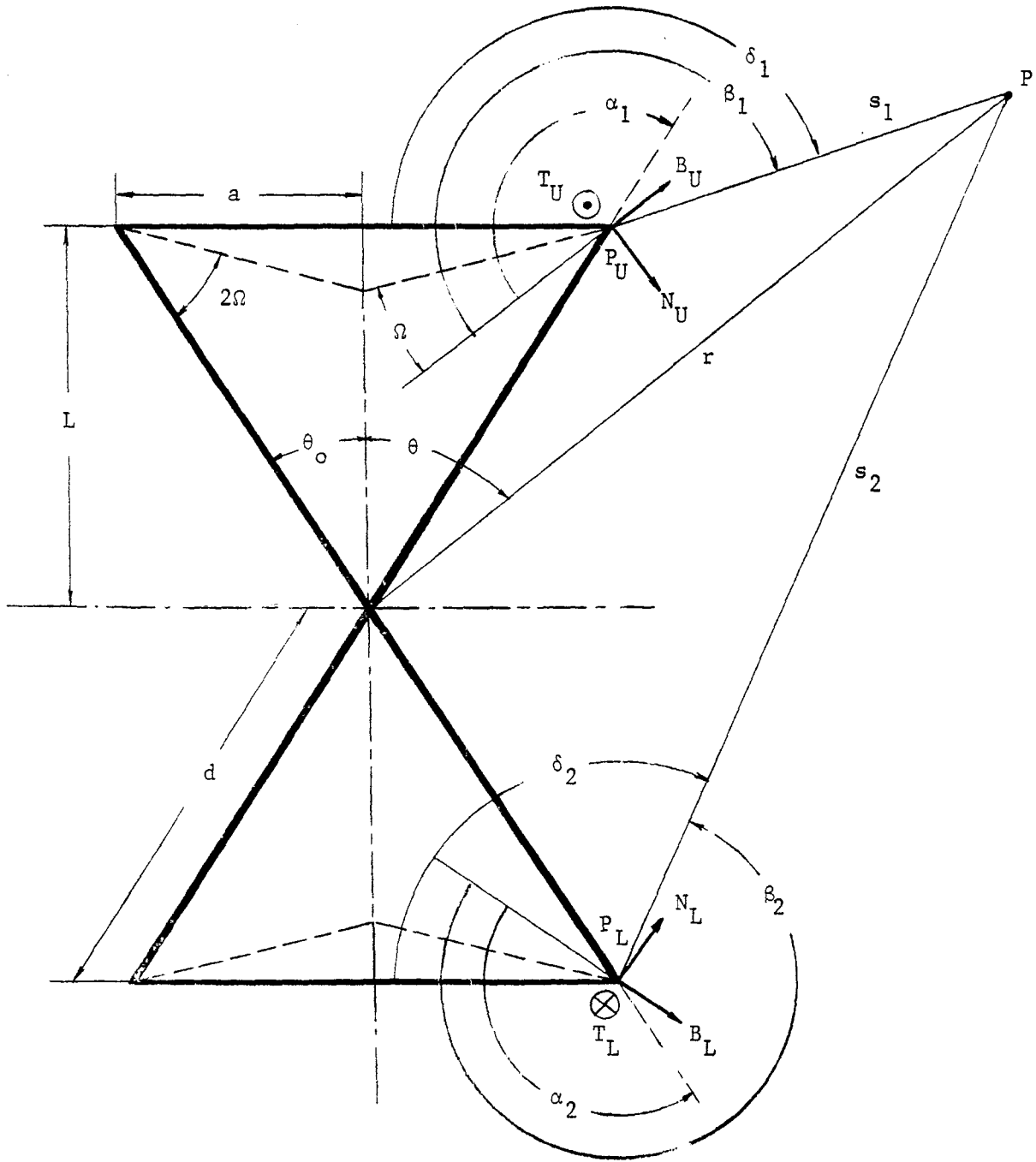
Figure 2. Diffraction Coordinate Systems.

Figure 3

16

Figure 4

$\theta_o = 45°$

17

Figure 5

18

Figure 6

$$|D_{1C}|(t - t_1)^{\frac{1}{2}})$$

$$-(V_{bo}f_o/\sin \theta)(1 - |D_{1U}|(t^* - t_1)^{\frac{1}{2}})$$

E_θ

t

t_1
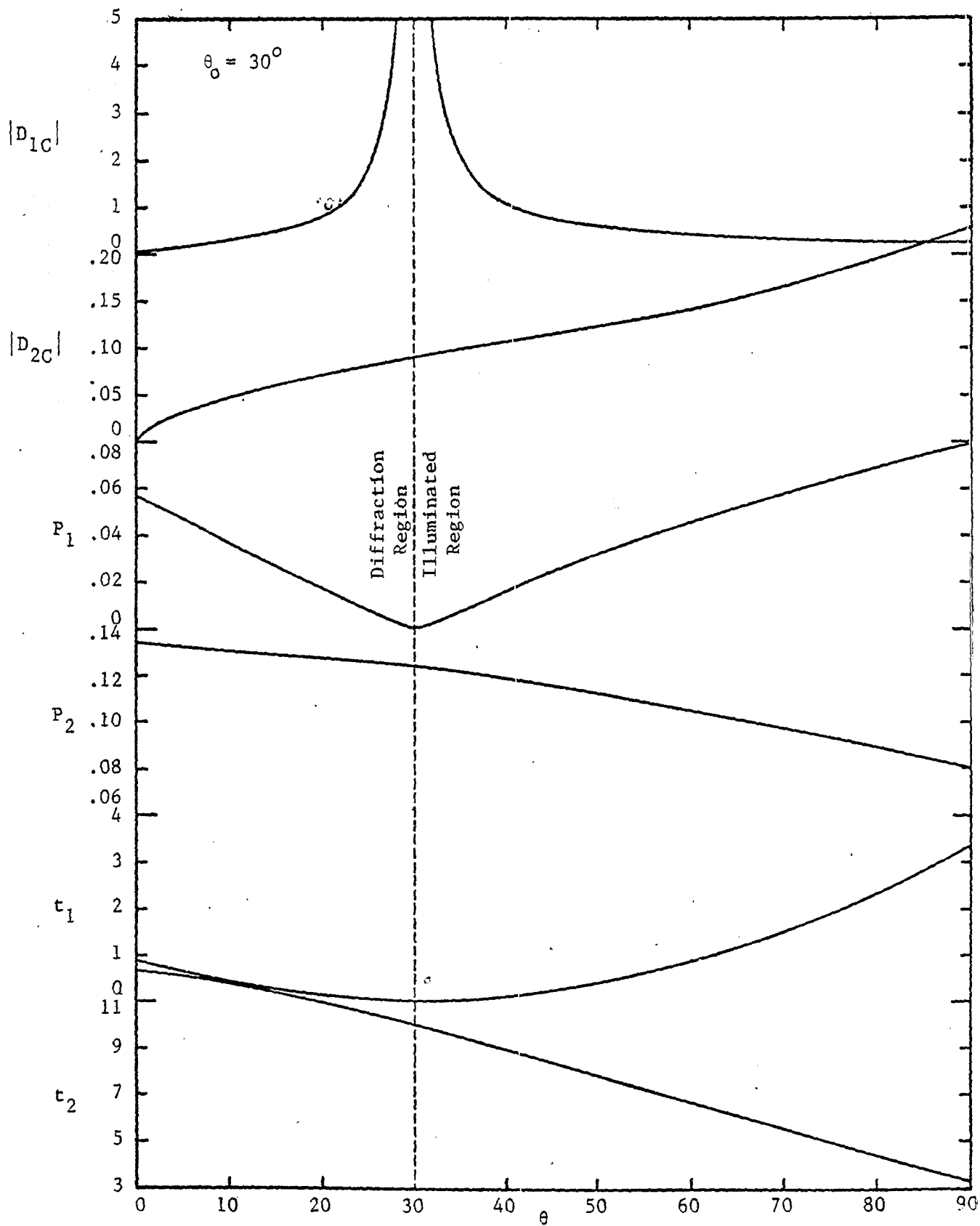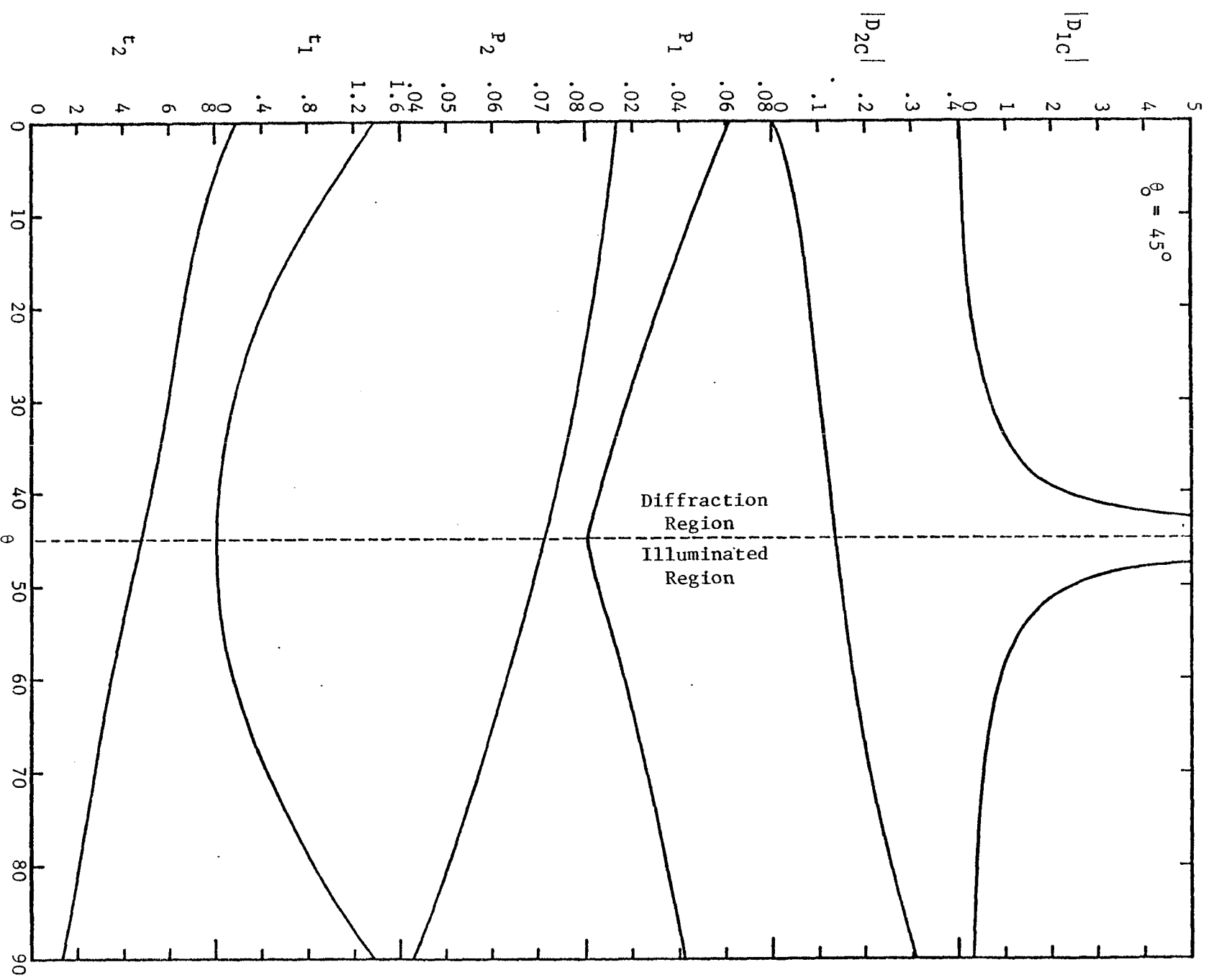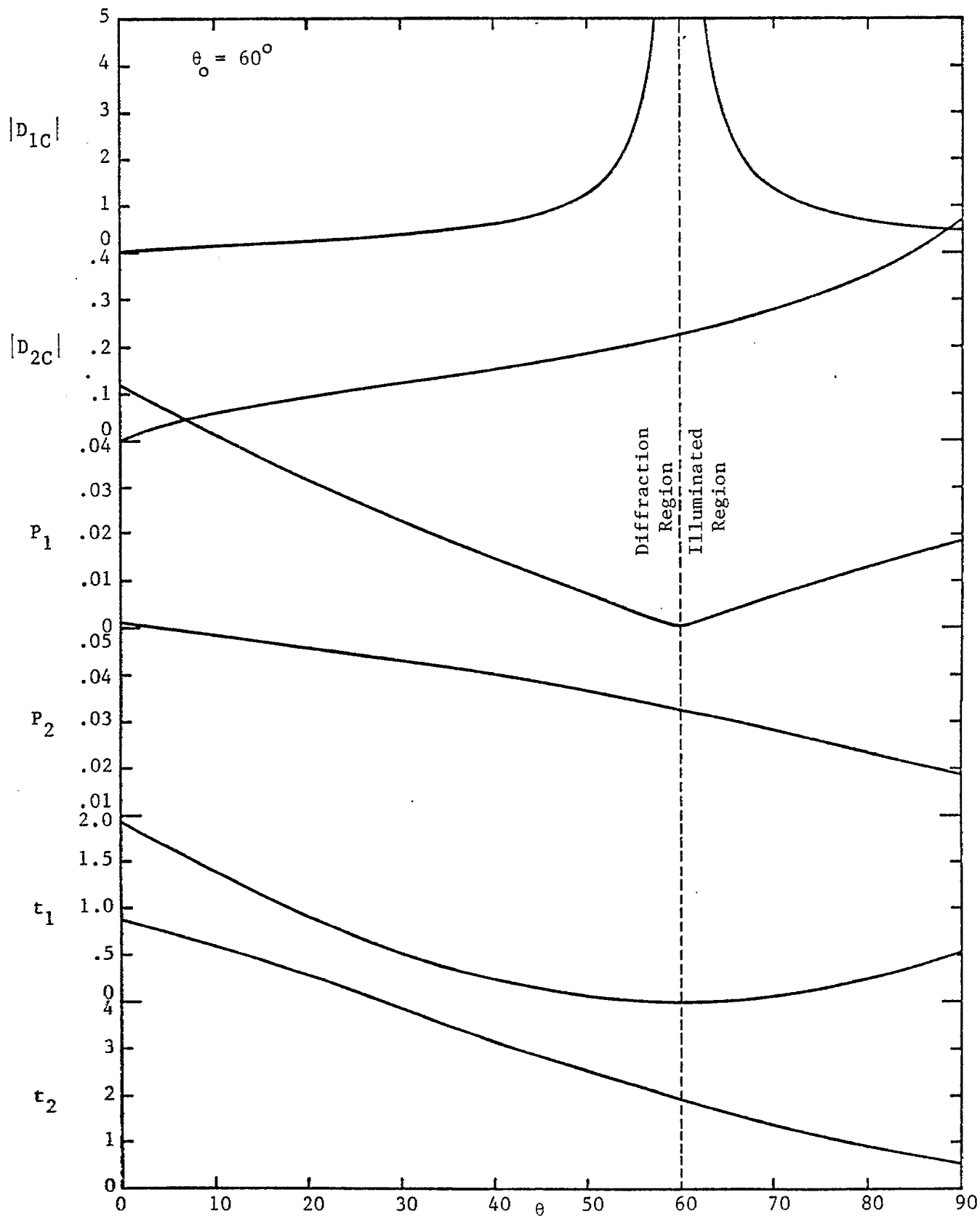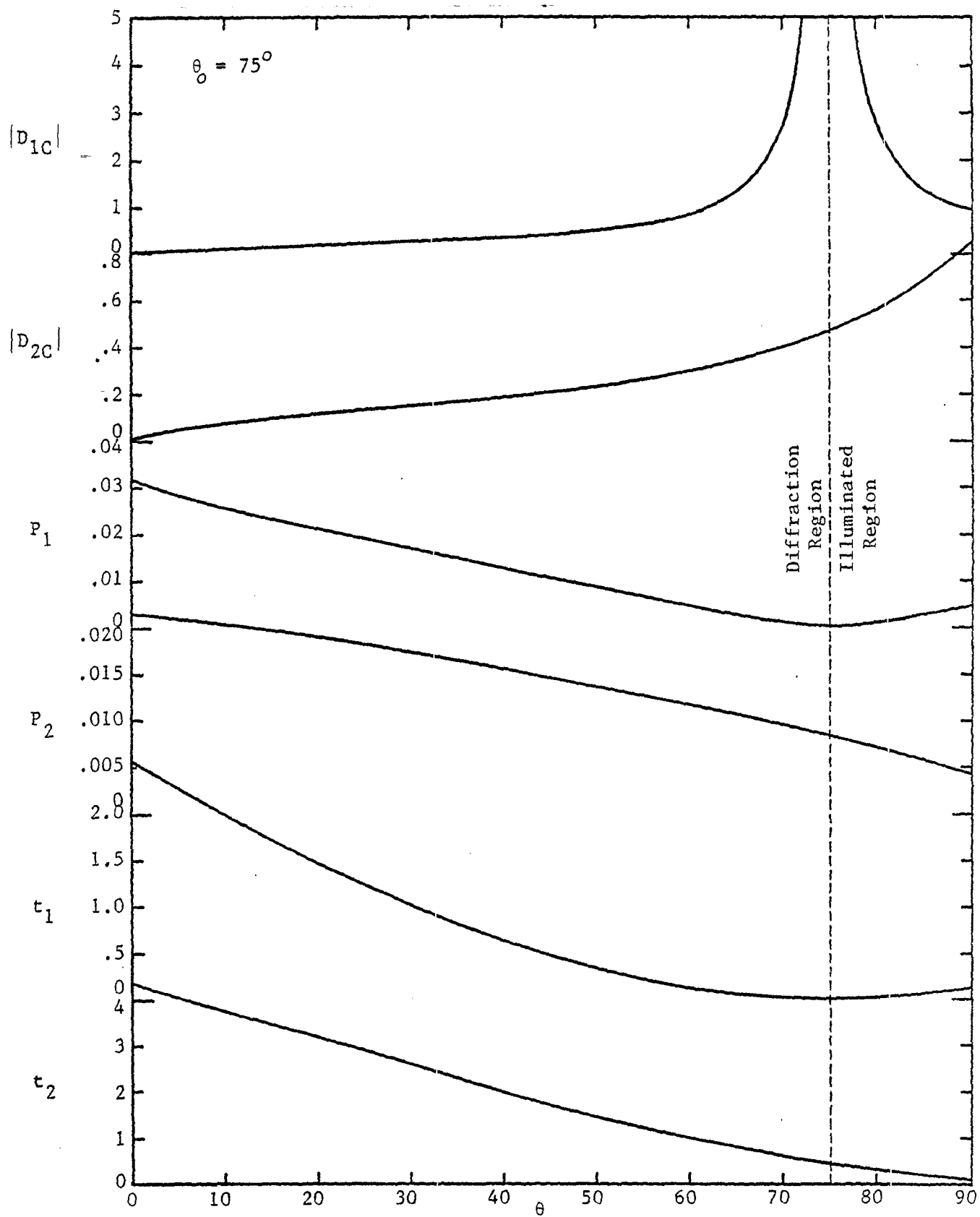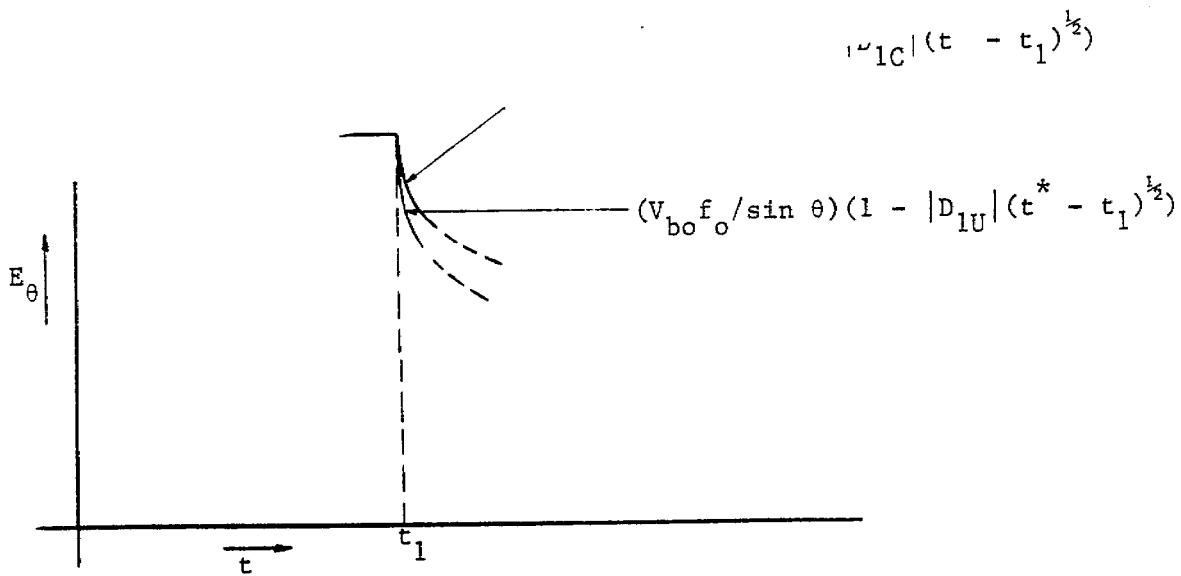
Figure 7a. Schematic Plot of Early Time Asymptotic Breaking Effect for
Observation Points in the Illuminated Region.

$$(V_{bo}f_o/\sin \theta)D_{1C}(t^* - t_1)^{\frac{1}{2}}$$

E_θ

$$(V_{bo}f_o/\sin \theta)D_{1U}(t^* - t_1)^{\frac{1}{2}}$$

t_1

t
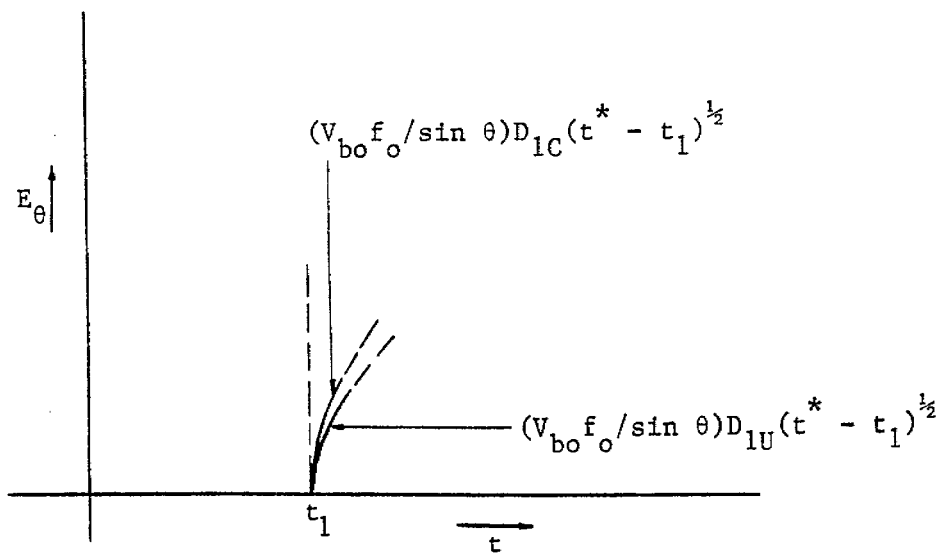
Figure 7b. Schematic Plot of Early Time Asymptotic Breaking Effect for
Observation Points in the Diffraction Region.

Acknowledgement

We thank Dr. C. E. Baum for his helpful comments and Mrs. G. Peralta for typing the manuscript.

References

1. Baum, C. E., "A Circular Conical Antenna Simulator," Sensor and Simulation Note 36, March 1967.

2. Baum, C. E., "Design of a Pulse-Radiating Dipole Antenna as Related to High-Frequency and Low-Frequency Limits," Sensor and Simulation Note 69, January 1969.

3. Keller, J. B., "Geometrical Theory of Diffraction," J. Opt. Soc. Am., $\underline{52}$. p. 116, 1962.

4. Sancer, M. I., and Varvatsis, A. D., "Geometrical Diffraction Solution for the High Frequency-Early Time Behavior of the Field Radiated by an Infinite Cylindrical Antenna With a Biconical Feed," Sensor and Simulation Note 129, May 1971.